NUCL SCI TECH (2019) 30:74
https://doi.org/10.1007/s41365-019-0600-8

Characterization of molten $2LiF–BeF_2$ salt impregnated into graphite matrix of fuel elements for thorium molten salt reactor

Hong-Xia Xu[1] · **Jun Lin**[1] · **Ya-Juan Zhong**[1] · **Zhi-Yong Zhu**[1] · **Yu Chen**[1] ·
Jian-Dang Liu[2] · **Bang-Jiao Ye**[2]

Received: 31 August 2018 / Revised: 15 October 2018 / Accepted: 20 October 2018 / Published online: 9 April 2019

Abstract The impregnation behavior of molten $2LiF–BeF_2$ (FLiBe) salt into a graphite matrix of fuel elements for a solid fuel thorium molten salt reactor (TMSR-SF) at pressures varying from 0.4 to 1.0 MPa was studied by mercury intrusion, molten salt impregnation, X-ray diffraction, and scanning electron microscopy techniques. It was found that the entrance pore diameter of the graphite matrix is less than 1.0 μm and the contact angle is about 135°. The threshold impregnation pressure was found to be around 0.6 MPa experimentally, consistent with the predicted value of 0.57 MPa by the Washburn equation. With the increase of pressure from 0.6 to 1.0 MPa, the average weight gain of the matrix increased from 3.05 to 10.48%, corresponding to an impregnation volume increase from 2.74 to 9.40%. The diffraction patterns of FLiBe are found in matrices with high impregnation pressures (0.8 MPa and 1.0 MPa). The FLiBe with sizes varying from tens of nanometers to a micrometer mainly occupies the open pores in the graphite matrix. The graphite matrix could inhibit the impregnation of the molten salt in the TMSR-SF with a maximum operation pressure of less than 0.5 MPa.

Keywords Molten salt reactor · FLiBe · Impregnation · Graphite matrix

1 Introduction

A molten salt reactor (MSR) is one of the most promising candidates for Generation IV reactors and has attracted more attention due to its unique recyclable fuel capabilities and safety characteristics [1–7]. A solid fuel thorium molten salt reactor (TMSR-SF) is a new MSR design proposed by the Shanghai Institute of Applied Physics (SINAP) in 2011 [4, 8]. The first TMSR-SF under R&D is a 10 MW liquid-fluoride molten salt (a eutectic mixture of $2LiF–BeF_2$)-cooled and graphite-moderated experimental reactor. The inlet and outlet temperatures are maintained at 600 °C and 628 °C, respectively. The maximum operation pressure of the $2LiF–BeF_2$ coolant is less than 0.5 MPa [9]. The reactor uses spherical fuel elements which are made of a graphite matrix and tri-isotropic (TRISO)-coated particle (CP) [8, 10]. These fuel elements were originally developed for high-temperature gas-cooled reactors (HTGRs) [11–14]. To use the fuel elements in TMSR-SF, the graphite matrix must be in direct contact with the molten salt. Owing to the porous nature of graphite, the molten salt may penetrate the pores of the graphite under high-pressure environments. The impregnation of graphite with molten salt has been studied and reported as early as the 1950s, when Oak Ridge National Laboratory (ORNL) in the USA conducted the impregnation of graphite with molten $LiF–BeF_2–UF_4$ salt in order to study the

---

This work was supported by the Thorium Molten Salt Reactor Nuclear Energy System under the Strategic Priority Research Program of the Chinese Academy of Sciences (No. XDA02030000), the Frontier Science Key Program of the Chinese Academy of Sciences (No. QYZDY-SSW-JSC016) and the State Key Laboratory of Particle Detection and Electronics (No. SKLPDE-KF-201811).

✉ Hong-Xia Xu
xuhongxia@sinap.ac.cn

[1] Center for Thorium Molten Salt Reactor System, Shanghai Institute of Applied Physics, Chinese Academy of Sciences, Shanghai 201800, China

[2] State Key Laboratory of Particle Detection and Electronics, University of Science and Technology of China (USTC), Hefei 230026, China

compatibility of molten salt with the graphite and select the type of graphite [15–18] to be used in MSR. Their studies [15–18] suggested that the impregnation of graphite with molten salt is closely related to the pressure environment and pore diameter of graphite. In addition, they reported that the impregnation of graphite with the molten fluoride salt is restricted by the surface tension (approximately 0.200 N/m) if the entrance pore is less than 1 μm [18]. Previous studies [17, 19, 20] have reported that the impregnation of graphite with molten salt may change the coefficient of thermal expansion and increase the damage rate for graphite. It is therefore essential to determine the impregnation behavior of molten salt into a graphite matrix of fuel elements.

In the present study, the impregnation behavior of molten FLiBe into a graphite matrix at high temperatures was investigated. Mercury intrusion was performed to determine the pore size distribution of the graphite matrix. The sessile drop method was used to measure the contact angle between the molten FLiBe salt and the graphite matrix. Using combinations of these results, the threshold impregnation pressure of the molten salt into the graphite matrix was calculated with the Washburn equation. The impregnation amounts of the molten FLiBe salt under pressures varying from 0.4 to 1.0 MPa in the graphite matrix were obtained. X-ray diffraction (XRD) and scanning electron microscopy (SEM) coupled with energy dispersive X-ray spectrometry (EDS) were used to characterize the phase and distribution of the molten FLiBe salt in the graphite matrix after impregnation, respectively.

2 Experimental

The graphite matrix comprises of 64% natural flake graphite, 16% graphitized coke, and 20% phenol resin binder, similar to that of the German A3-3 graphite [11–14]. To prepare the graphite matrix, the raw materials were well mixed and the mixture was compressed into spherical balls of 6 cm in diameter, followed by carbonization at 800 °C and purification at 1900 °C. Details about the fabrication procedure of the graphite matrix were reported in our previous study [21]. The prepared graphite matrix sphere had a density of 1.74 ± 0.01 g/cm^3 and an anisotropic factor of approximately 1.03, similar to that of the A3-3.

The graphite matrix sphere was then machined into samples with sizes of $\Phi10$ mm × 15 mm and $\Phi10$ mm × 20 mm for the mercury intrusion and molten salt impregnation experiments, respectively. The mercury intrusion was performed with an AutoPore IV 9500 mercury intrusion porosimeter [22] in the incremental mode, from which the open porosity, mercury intrusion curve, and pore diameter distribution of the graphite matrix could be obtained. The samples with dimensions of $\Phi10$ mm × 15 mm were degassed before the mercury intrusion experiment.

The molten FLiBe salt impregnation experiment [9] was performed in a homemade autoclave, the schematic structure of which can be seen in Fig. 1a. It consists of a graphite crucible placed inside the autoclave, a sample holder comprising one rod, and two or three graphite plates according to the number of samples. The pressures of the autoclave could be varied from 0.4 to 1.0 MPa, controlled by the pressure of the argon cover gas. The graphite samples with dimensions of $\Phi10$ mm × 20 mm were held between the two graphite plates in the sample holder; the schematic structure of the assembled samples is shown in Fig. 1b. The samples were partially degassed by heating at 400 °C under vacuum for 4 h, according to previous studies [9, 23]. The weights of the samples before and after the impregnation tests were measured using an analytical balance (METTLER TOLEDO MS105DU), located in the glove box. During impregnation, three graphite samples were completely submerged in the molten FLiBe salt at 650 °C for 20 h under each pressure. After the impregnation, the graphite samples were removed from the molten salt and weighted. The weight gain ratio γ for each sample was calculated using the following equation:

$$\gamma = \frac{W_1 - W_0}{W_0}, \tag{1}$$

where W_0 and W_1 are the sample weights before and after molten salt impregnation, respectively.

In addition, the intrusion volume fraction v was calculated using the following equation:

$$v = \frac{\gamma \times \rho_G}{\rho_S}, \tag{2}$$

where ρ_S and ρ_G are the density of the molten FLiBe salt (approximately 1.94 g/cm^3 at 650 °C [24]) and the graphite matrix (1.74 g/cm^3), respectively.

The contact angle between the molten FLiBe salt and the graphite matrix at 650° was measured using the sessile drop technique using a OCA15LHT goniometer [25–27]. For this measurement, the graphite matrix sample with a size of $\Phi10$ mm × 2 mm was placed on a graphite disk-shaped substrate, and the solid FLiBe salt with a size of $\Phi5$ mm × 6 mm was placed on top of the graphite disk (see Fig. 2). The chamber was purged with argon (99.99%) before the sample was heated to the required temperature. SCA20 software was used to control the furnace and record the video captured by the CCD camera.

Crystal phase structures of the specimens before and after impregnation were characterized using a XRD spectrometer. The diffractometer used Cu k_α radiation

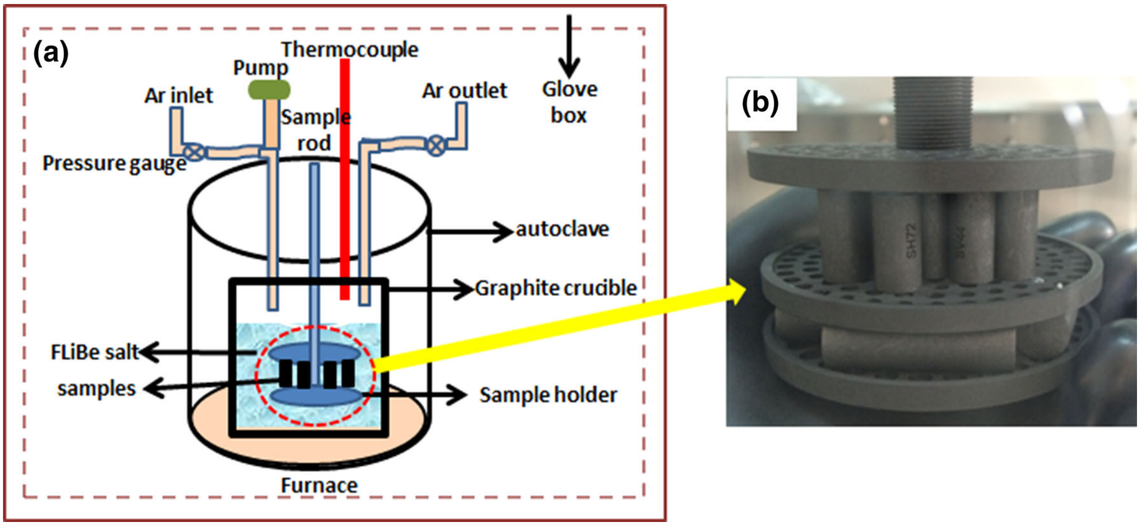

Fig. 1 (Color online) **a** Schematic structure of the molten salt impregnation experiment device and **b** samples assembled in the sample holder

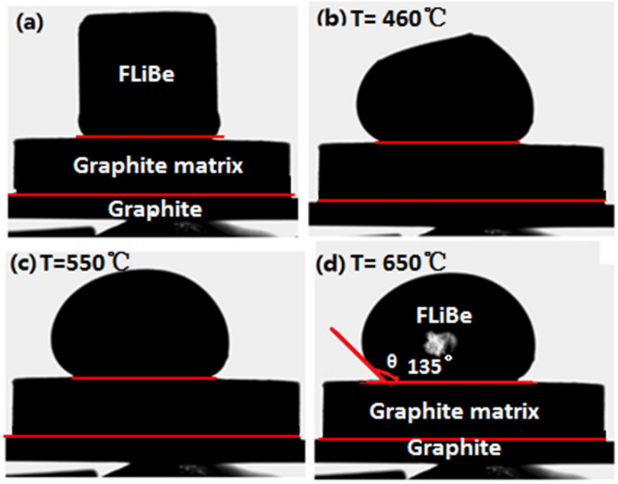

Fig. 2 Sessile drop profiles of contact angle (θ_{salt}) between the molten FLiBe salt and graphite

($\lambda \sim 0.154$ nm, 40 kV, and 40 mA) with a scanning angle ranging from 20° to 90° on a 2θ scale.

The distribution of the FLiBe at the surface of the impregnated graphite matrix was examined by using SEM (Zeiss: Merlin compact) with EDS.

3 Results and Discussion

3.1 Mercury and molten salt impregnation into the graphite matrix

Previous ORNL studies [15–18] suggested that the impregnation of graphite with molten salt is closely related to the pressure, surface tension, contact angle, and pore diameter of graphite. The capillary pressure of the molten salt determined by the entrance pore size can be described by the Washburn equation [Eq. (3)] [28]:

$$p = -\frac{4\gamma\cos\theta}{\delta}, \quad (3)$$

where p is the capillary pressure or pressure difference on the interface between the mercury and gas inside the pore of the graphite, γ is the surface tension, θ is the contact angle, and δ is the entrance diameter of the penetrated pores.

The contact angle is a crucial indicator for providing data on the wetting characteristic of the molten salt into the graphite due to its close relationship with the impregnation. A previous study showed that it has a surface tension (γ_{salt}) of about 0.200 N/m and a contact angle (θ_{salt}) with graphite of 147 ± 12° at 650 °C [18]. The sessile drop method was used to determine the contact angle by viewing the drop profile shown in Fig. 2. It can be clearly seen that the FLiBe gradually melted into a liquid drop when the temperature was increased to its melting point (approximately 458 ± 1 °C [24, 29]) under an argon atmosphere. The drop shape remained unchanged even when the temperature was increased to 650 °C. For the present measurement, θ_{salt} determined by the goniometer eyepiece was approximately 135 ± 2° (Fig. 2), which is consistent with the value reported above, indicating the non-wetting characteristics of the molten salt to the graphite under a normal atmospheric environment. However, the θ_{salt} determined here is close to the minimum value obtained by the previous measurement [18], which may be ascribed to the difference in the flatness of the graphite. Several factors [18, 19, 25] can affect the contact angle measured by the sessile drop method, such as the content of H_2O traces in the purge gas and surface flatness of the substrate. Since the graphite has a natural porous structure, it is very difficult to prepare an ideal flat surface for consistent measurements.

The pore diameter is another critical indicator for determining the impregnation of graphite with molten salt. Mercury intrusion porosimetry was used to determine the pore size (with the accuracy of the pore diameter measurement being approximately ± 0.1%) distribution and porosity (pore volume fraction) of three graphite samples in this test. The surface tension (γ_{Hg}) and contact angle (θ_{Hg}) between mercury and graphite are reported to be about 0.485 N/m and 130.0° [30], respectively. The mercury intrusion results are shown in Fig. 3, in which the changes in the cumulative mercury intrusion with pressure and the distribution of the pore diameter for the graphite matrix are given in Fig. 3a, b, respectively.

As can be seen from Fig. 3a, the mercury could not be impregnated into the graphite matrix when the pressure was very low at the beginning. However, the cumulative mercury intrusion detected sudden increases when the pressure exceeded a certain value (approximately 1.3 MPa), suggesting that the pores of the graphite were filled with mercury after the pressure exceeded the threshold value. The entrance pore diameter for the graphite matrix was calculated according to the Washburn equation and its distribution is given in Fig. 3b. As can be seen, the distribution of the entrance pore diameter is rather narrow. The maximum entrance pore diameter for the graphite matrix was approximately 1.0 μm, corresponding to the threshold pressure (1.3 MPa).

According to the Washburn equation, the pressure is the controlling factor for salt penetration as long as the wetting characteristic of the graphite and salt is not altered. The threshold impregnation pressure calculated using Eq. 3 was approximately 0.57 MPa for an entrance pore size of 1.0 μm, indicating that if the operating pressure is lower than 0.57 MPa, the molten salt should not impregnate the graphite matrix. In fact, the maximum operating pressure of the molten FLiBe salt designed for TMSR-SF is less than 0.5 MPa, which suggests that the molten FLiBe will not impregnate fuel elements under normal operating conditions in TMSR-SF without regarding the irradiation conditions.

The obtained weight gain ratio γ of the graphite matrix exposed to the FLiBe under various pressures after impregnation is shown in Fig. 4. As can be seen, the average weight gain ratio of the graphite matrix impregnated at pressures lower than 0.6 MPa is zero, indicating no FLiBe permeation occurred. With increasing the pressure from 0.6 to 1.0 MPa, the average weight gain ratio γ of the matrix increased from 3.05 to 10.48% compared to its original weight, corresponding to a volume fraction v increase from 2.74 to 9.40%. The results indicate that the

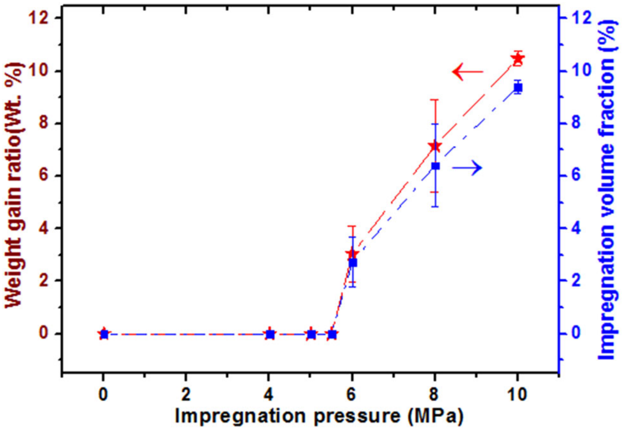

Fig. 4 Weight gain ratio and impregnation volume fraction of samples with pressure increased from 0.4 to 1.0 MPa

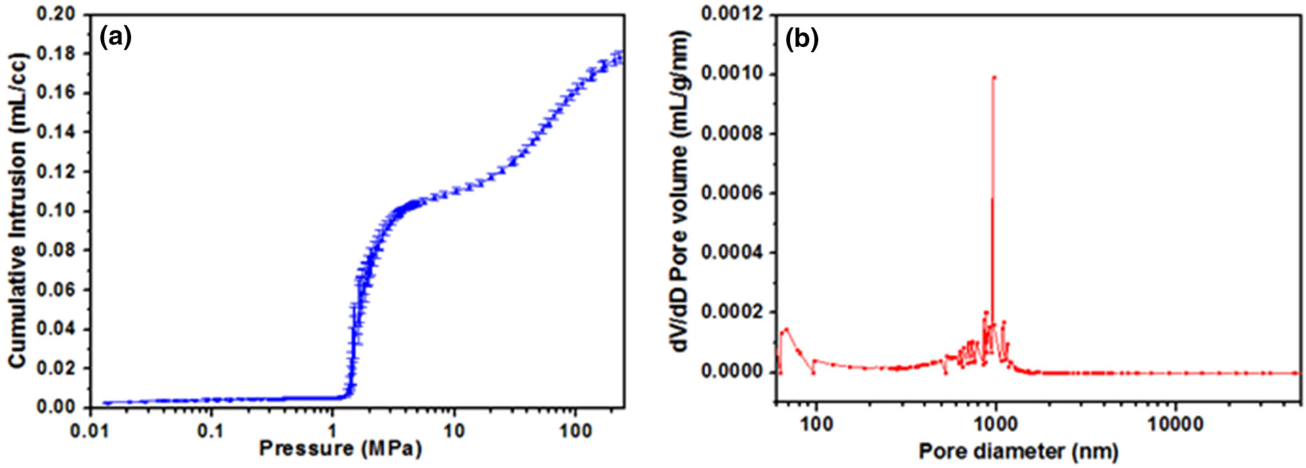

Fig. 3 Results of mercury intrusion experiments: **a** cumulative mercury intrusion curve and **b** distribution of the entrance pore diameters for graphite matrix

threshold pressure for the FLiBe impregnation of the graphite matrix is between 0.55 and 0.6 MPa, which agrees with the value of 0.57 MPa calculated using the Washburn equation for an entrance pore size of 1.0 μm in diameter and a contact angle of 135°.

3.2 Phase characterization of matrix

In order to evaluate the influence of molten salt impregnation on crystallite phase structure, the XRD patterns of the matrix specimens before and after impregnation are shown in Fig. 5. As can be seen clearly, six characteristic graphite diffraction peaks located at approximately $2\theta = 26.44°$ (002), 42.23° (100), 44.40° (101), 54.56° (004), 77.38° (110), and 83.49° (112) [31, 32] appear in all the specimens. In addition, there is no obvious change in both the peak location and the full width at half maximum (FWHM) of the (002) diffraction for each sample, suggesting that FLiBe impregnation does not change the crystallinity of the matrix. It should be noted that this result is completely different from the previous study [19], in which the stacking order of graphite was found to be improved after impregnation with molten salt. The reason for this may be due to the molten FLiBe salt being impregnated into the pores rather than migrating inside the graphite crystal lattice in our experiment. However, for matrix samples impregnated with pressures of 0.8 MPa and 1.0 MPa, new diffraction peaks assigned to the FLiBe phase at 2θ, ranging from 20° to 50°, appear.

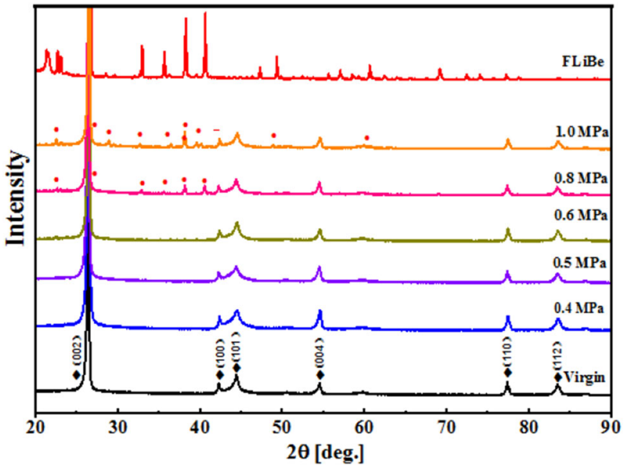

Fig. 5 XRD pattern of the graphite matrix with various impregnation pressures; black diamond indicates graphite, red circle indicates FLiBe. (Color figure online)

The interlayer spacing d_{002}, the graphitization degree $\bar{g}$, and the mean dimension of the crystallite perpendicular to the diffracting plane (002) L_c derived from the XRD patterns can be calculated using the Bragg diffraction equation (Eq. 4), Mering-Maire equation (Eq. 5), and Scherrer equation (Eq. 6), respectively [31–33]:

$$d_{002} = \frac{\lambda}{2\sin\theta}, \tag{4}$$

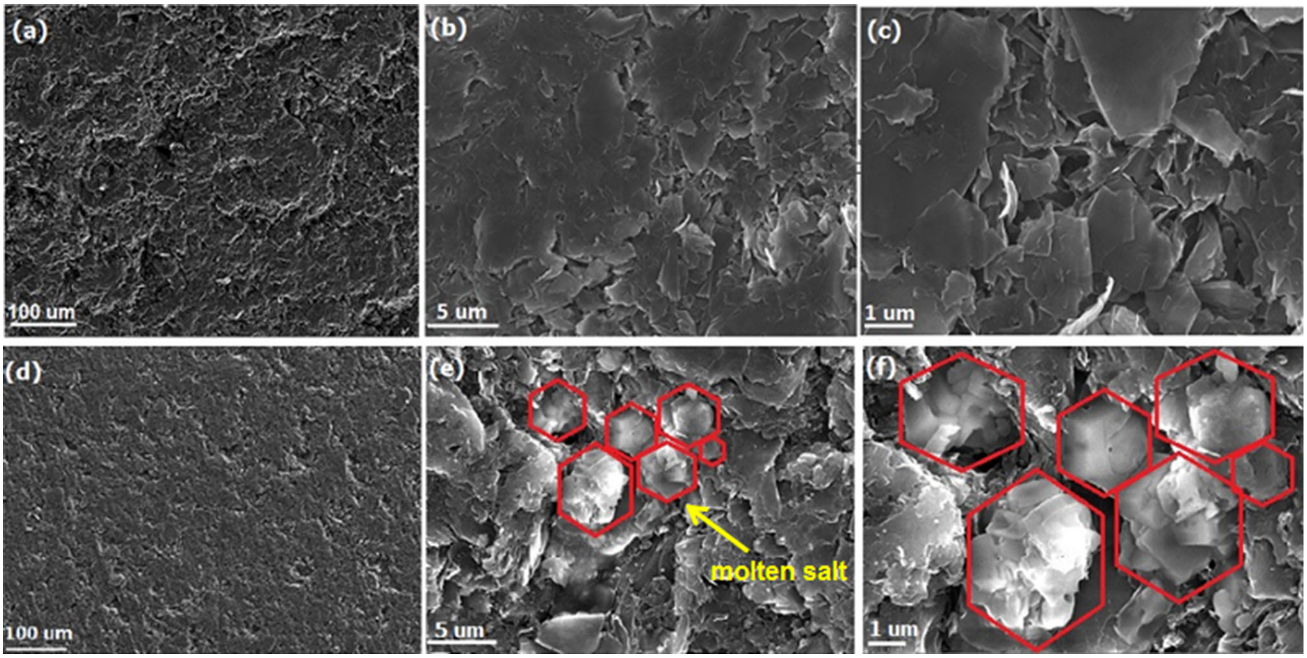

Fig. 6 Surface SEM images of virgin and impregnated graphite matrix: **a–c** are virgin samples under different magnifications, **d–f** show the impregnated specimen with 0.6 MPa under different magnifications

$$\bar{g} = \frac{0.3440 - d_{002}}{0.3440 - 0.3354}, \quad (5)$$

$$L_c = \frac{0.9\lambda}{\beta_{002} \cos \theta_{002}}, \quad (6)$$

where λ, θ, and β are the wavelength of the X-rays, the Bragg angle, and the diffraction peak width, respectively.

The interlayer spacing d_{002}, graphitization $\bar{g}$, and the mean crystallite size L_c of the graphite crystallite before impregnation are about 0.3370 nm, 81.1%, and 40 nm, respectively. After FLiBe impregnation, no obvious changes in the phase parameters of the matrix were observed, revealing that the impregnation of the molten FLibe salt does not damage the crystallite structure of the graphite matrix.

3.3 Distribution and morphology of FLiBe salt in the graphite matrix

Radiographic examinations of the MSRE graphite [15, 16] showed only skin-like permeation or shallow-surface (1.27 mm) impregnation of the salt in the specimens. However, He et al. [19] recently reported that there was very little difference between the molten salt content at the center and at the surface of the impregnated samples. In an attempt to determine the FLiBe distribution in the graphite matrix, SEM with EDS examinations was performed for the surface of the salt-permeated specimens.

The surface SEM results of the virgin matrix are shown in Fig. 6a–c, which reveal that the matrix has many large graphite lamellas and irregular pores with sizes less than 1.0 μm located at the surface or interfaces between the graphite crystallites. Some pores seem to have a hexagonal shape, which should not introduce a significant error when calculating the capillary pressure using the Washburn equation. Figure 6d–f shows the surface SEM images of the matrix after impregnation with a pressure of 0.6 MPa. It was found that the impregnated matrix has a bright contrast throughout the specimen, and some hundreds of nanometers to several micrometer-sized FLiBe particles were located at the open pores, which is very similar to the

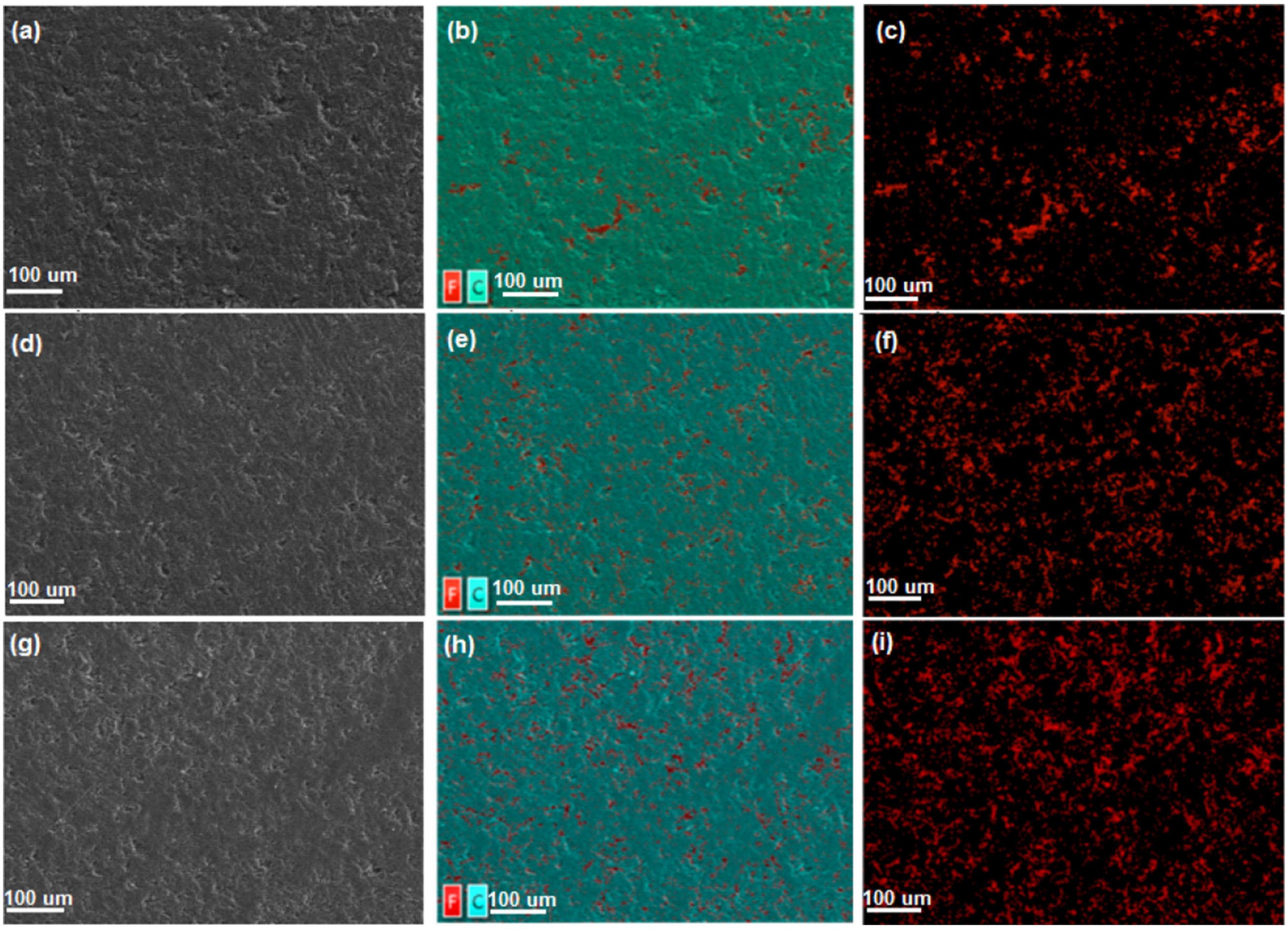

Fig. 7 (Color online) FLiBe distribution on the surface of impregnated specimens with various pressures from 0.6 to 1.0 MPa **a–c**, **d–f** and **g–i** are the SEM image, EDS image (blue and red color represent the distribution of C and F, respectively), and the distribution of F under 0.6 MPa, 0.8 MPa, and 1.0 MPa impregnated graphite matrix, respectively

distribution of the fluoride molten salt in other kinds of nuclear graphite [9, 19, 34, 35].

The distributions of the molten salt on the surface of the impregnated samples with pressures increasing from 0.6 to 1.0 MPa obtained by EDS together with SEM are shown in Fig. 7. The molten FLiBe salt is easy to distinguish from the matrix because it is a brilliant white color when observed by SEM, as shown in Fig. 6. As can be seen from the comparison of the SEM and EDS images of the graphite matrix, the distributions of the molten salt on the graphite surface have a net-like structure and are superposed with the opening pores; this suggests that the pore shape structure of the graphite determines the distribution of FLiBe. In addition, with the impregnation pressure increased from 0.6 to 1.0 MPa, there is a significant increase in the amount of salt observed on the graphite surface, and the size of the vacant area reduces, indicating that more opening pores are occupied by the molten salt due to the higher impregnation pressure. This is in agreement with the weight gain measurement.

The maximum operation pressure in the TMSR-SF design is expected to be below 0.5 MPa. Therefore, it is confirmed that the molten salt should not be impregnated into the graphite matrix in case the matrix structure is not alerted by the reactor environment. The present work reveals that a graphite matrix with an entrance pore size less than 1.0 μm in diameter has a high resistance to molten salt impregnation and could be a promising structural material for TMSR-SF fuel elements. However, if for some reason, such as neutron irradiation, the entrance pore size of the graphite matrix changes, the impregnation behavior of the FLiBe salt in the graphite matrix may change. It is therefore very important to investigate the post-irradiation behavior of the graphite matrix, which is under investigation in our institute.

4 Conclusion

The mercury and molten FLiBe salt impregnation into a graphite matrix of fuel elements prepared for TMSR-SF were performed under various pressures. The phase and surface morphology of the FLiBe impregnated into the graphite matrix were characterized by XRD and SEM analyses. No graphite matrix was impregnated with molten salt at impregnation pressures below 0.55 MPa, which agrees well with the calculated threshold pressure of 0.57 MPa determined by the Washburn equation with an entrance pore diameter of 1.0 μm and a contact angle of 135°. As the impregnation pressure increased from 0.6 to 1.0 MPa, the molten FLiBe salt was forced to penetrate the open pores of the matrix, resulting in a weight gain increase from 3.05 to 10.48%. The XRD diffraction patterns unique to FLiBe salt were observed in the graphite matrix with impregnation pressures of 0.8 MPa and 1.0 MPa. The surface morphology of the impregnated samples observed by SEM with EDS shows that the FLiBe was mainly distributed in the pores of the matrix with pore sizes in the range of tens of nanometers to several micrometers. The distributions of the molten FLiBe salt impregnated into samples at higher pressure were irregular, which is closely related to the original pore shape of the graphite matrix.

References

1. T. Abram, S. Ion, Generation-IV nuclear power: a review of the state of the science. Energy Policy **36**, 4323–4330 (2008). https://doi.org/10.1016/j.enpol.2008.09.059
2. R.O. Scarlat, P.F. Peterson, The current status of fluoride salt cooled high temperature reactor (FHR) technology and its overlap with HIF target chamber concepts. Nucl. Inst. Methods Phys. Res. Sect. A **733**, 57–64 (2014). https://doi.org/10.1016/j.nima.2013.05.094
3. G.L. Yoder, A. Aaron, B. Cunningham et al., An experimental test facility to support development of the fluoride-salt-cooled high temperature reactor. Ann. Nucl. Energy **64**, 511–517 (2014). https://doi.org/10.1016/j.anucene.2013.08.008
4. J. Serp, M. Allibert, O. Benes et al., The molten salt reactor (MSR) in generation IV: overview and perspectives. Prog. Nucl. Energy **77**, 308–319 (2014). https://doi.org/10.1016/j.pnucene.2014.02.014
5. A. Acir, Neutronic analysis of the laser inertial confinement fusion-fission energy (LIFE) engine using various thorium molten salts. J. Fusion Energy **32**(6), 634–641 (2013). https://doi.org/10.1007/s10894-013-9628-7
6. Y. Zhong, X. Yang, D. Ding et al., Numerical study of thedynamic characteristics of a single-layer graphite core in a thorium molten salt reactor. Nucl. Sci. Tech. **29**, 141 (2018). https://doi.org/10.1007/s41365-018-0488-8
7. X. Yang, Y.T. Gao, Y. Zhong et al., Stress analysis of the TMSR graphite component under irradiation conditions. Nucl. Sci. Tech. **29**, 173 (2018). https://doi.org/10.1007/s41365-018-0516-8
8. Z.M. Dai, Thorium molten salt reactor nuclear energy system (TMSR), in *Molten Salt Reactors and Thorium Energy*, pp. 531–540 (2017). https://doi.org/10.1016/b978-0-08-101126-3.00017-8
9. H. Tang, W. Qi, Z.T. He et al., Infiltration of graphite by molten 2LiF–BeF$_2$ salt. J. Mater. Sci. **52**, 11346–11359 (2017). https://doi.org/10.1007/s10853-017-1310-4
10. K.J. Kruger, G.P. Ivens, Safety-related experiences with the AVR reactor, in *Proceedings of A Specialists' Meeting on Safety and Accident Analysis for Gas-cooled Reactors*. USA: Oak Ridge National Laboratory, IAEA-TECDOC-358, pp. 61–70 (1985)
11. J.J. Powers, B.D. Wirth, A review of TRISO fuel performance models. J. Nucl. Mater. **405**(1), 74–82 (2010). https://doi.org/10.1016/j.jnucmat.2010.07.030
12. Advances in high temperature gas cooled reactor fuel technology. Austria: Vienna. IAEA-TECDOC-1674 (2012)
13. C.H. Tang, Y.P. Tang, J.G. Zhu et al., Design and manufacture of the fuel element for the 10 MW high temperature gas-cooled reactor. Nucl. Eng. Des. **218**, 91–102 (2002). https://doi.org/10.1016/s0029-5493(02)00201-7

14. R.E. Schulze, H.A. Schulze, W. Rind, Graphitic Matrix Materials for Spherical HTR Fuel Elements. Germany, JUEL–1702 (1981)
15. R.B. Briggs, *Molten Salt Reactors Program Progress Report for Period from August 1, 1960 to February 28* (Oak Ridge National Laboratory, ORNL-3122, USA, 1961), pp. 93–95
16. R.B. Briggs, *Molten Salt Reactors Program Semiannual Progress Report for Period Ending February 28*. Oak Ridge National Laboratory, ORNL-3282, USA, 1962), pp. 90–94
17. H.G. MacPherson, *Molten-Salt Reactor Project: Quarterly Progress Report* (Oak Ridge National Laboratory, ORNL-2723, USA, 1959)
18. W.R. Grimes, E.G. Bohlmann, H.F. McDuffie et al., *Reactor Chemistry Division Annual Progress Report for Period Ending January 31* (Oak Ridge National Laboratory, ORNL-3591, USA, 1964), p. 39
19. Z. He, L. Gao, W. Qi et al., Molten FLiNaK salt infiltration into degassed nuclear graphite under inert gas pressure. Carbon **84**, 511–518 (2015). https://doi.org/10.1016/j.carbon.2014.12.044
20. P.R. Kasten, E.S. Bettis, W.H. Cook et al., Graphite behavior and its effects on MSBR performance. Nucl. Eng. Des. **9**(2), 157–195 (1969). https://doi.org/10.1016/0029-5493(69)90057-0
21. Y.J. Zhong, J.P. Zhang, J. Lin et al., Mesocarbon microbead based graphite for spherical fuel element to inhibit the infiltration of liquid fluoride salt in molten salt reactor. J. Nucl. Mater. **490**, 34–40 (2017). https://doi.org/10.1016/j.jnucmat.2017.04.003
22. AutoPore IV 9500 Operator's Manual V1.04, Micromeritics Instrument corporation, Part No. 950-42801-01 (August 2001)
23. Standard guide for impregnation of graphite with molten salt, Designation: D809116 (2017)
24. S. Cantor, J.W. Cooke, A.S. Dworkin et al., *Physical Properties of Molten-Salt Reactor Fuel, Coolant and Flush Salts* (Oak Ridge National Laboratory, ORNL-TM-2316, USA, 1968)
25. T.T. Chau, A review of techniques for measurement of contact angles and their applicability on mineral surfaces. J. Miner Eng. **22**(3), 213–219 (2009). https://doi.org/10.1016/j.mineng.2008.07.009
26. A.S. Dimitrov, P.A. Kralchevsky, A.D. Nikolov et al., Contact angle measurements with sessile drops and bubbles. J. Colloid Interface Sci. **145**(1), 279–282 (1991). https://doi.org/10.1016/0021-9797(91)90120-w
27. M.A. Duchesne, R.W. Hughes, Slag density and surface tension measurements by the constrained sessile drop method. Fuel **188**, 173–181 (2017). https://doi.org/10.1016/j.fuel.2016.10.023
28. E.W. Washburn, The dynamics of capillary flow. Phys. Rev. **117**(3), 273–283 (1921)
29. J.P.M. van der Meer, R.J.M. Konings, H.A.J. Oonk, Thermodynamic assessment of the LiF–BeF_2–ThF_4–UF_4 system. J. Nucl. Mater. **357**, 48–57 (2006). https://doi.org/10.1016/j.jnucmat.2006.05.042
30. A. Awasthi, Y.J. Bhatt, S.P. Garg, Measurement of contact angle in systems involving liquid metals. Meas. Sci. Technol. **7**, 753–757 (1996). https://doi.org/10.1088/0957-0233/7/5/005
31. T. Tanabe, K. Niwase, N. Tsukuda et al., On the characterization of graphite. J. Nucl Mater. **191–194**(A), 330–334 (1992)
32. S.F. Bartram, E.F. Kaelble, *Handbook of X-Rays for Diffraction, Emission, Absorption and Microscopy* (McGraw-Hill, New York, 1967), pp. 17.1–17.18
33. C.L. Qian, G.Z. Zhou, Q.Z. Huang, Graphitization measurement of carbon materials by X-ray diffraction. J. Cent. South Univ. Technol. **3**, 285–288 (2001)
34. J.L. Song, Y.L. Zhao, J.P. Zhang et al., Preparation of binderless nanopore-isotropic graphite for inhibiting the liquid fluoride salt and Xe^{135} penetration for molten salt nuclear reactor. Carbon **79**, 36–45 (2014). https://doi.org/10.1016/j.carbon.2014.07.022
35. V. Bernardet, S. Gomes, S. Delpeux et al., Protection of nuclear graphite toward fluoride molten salt by glassy carbon deposit. J. Nucl. Mater. **384**, 292–302 (2009). https://doi.org/10.1016/j.jnucmat.2008.11.032